

Comparative performance investigation of mono- and poly-crystalline silicon photovoltaic modules for use in grid-connected photovoltaic systems in dry climates

Saeed Edalati ^a, Mehran Ameri ^{b,*}, Masoud Iranmanesh ^a

^a Department of Energy, Institute of Science and High Technology and Environmental Sciences, Graduate University of Advanced Technology, Kerman, Iran

^b Department of Mechanical Engineering, Shahid Bahonar University of Kerman, Kerman, Iran



HIGHLIGHTS

- Output energy from two PV technology types (mc-Si and p-Si) are compared.
- Experimental measured data have been checked for consistency and have been validated.
- Annual average of capacity factor is found about 23.20% and 23.81% for mc-Si and p-Si, respectively.
- Effect of an increase in module temperature on output power from two PV technology types has been observed.
- Performance parameters of a grid-connected PV power plant have been experimentally studied during twelve months.

ARTICLE INFO

Article history:

Received 4 May 2015

Received in revised form 16 August 2015

Accepted 15 September 2015

Available online 29 September 2015

Keywords:

PV power plant

Grid-connected system

Performance evaluation

Capacity factor

ABSTRACT

In this study, the design and performance of a real 11.04 kWp grid connected photovoltaic (PV) system is investigated. This plant is composed of two types of 5.52 kWp common crystalline PV technology with almost similar characteristics. The PV power plant is established in an industrial sector of Kerman, Iran which experiences the same fluctuations in solar irradiance and ambient temperature for both types of monocrystalline silicon (mc-Si) and polycrystalline silicon (p-Si) PV modules. For experimental investigation of the plant, all meteorological and performance data of PV power plant are acquired by means of dedicated systems during July 2013 to June 2014. Thus, in this pioneer study, performance evaluations of two types of crystalline PV technology are studied, and as a part of considerations in the PV power plant design, the output power from p-Si PV modules is found greater. The annual average daily final yield (Y_f), performance ratio (PR), and capacity factor (CF) for mc-Si are found to be 5.24 kW h/kWp day, 80.81%, and 23.20%, respectively. Furthermore, Y_f , PR, and CF for p-Si are estimated as 5.38 kW h/kWp day, 82.92%, and 23.81%, respectively.

© 2015 Elsevier Ltd. All rights reserved.

1. Introduction

Nowadays, renewable energy has a controversial role in the sustainable development of countries. Moreover, a growing number of developed and developing countries have established targets for this clean kind of energy in order to reduce environmental issues of fossil energy resources such as greenhouse gas emissions, climate change, and global warming. Many sources of renewable energy such as Wind power, Hydropower, Solar energy, Biomass,

Biofuels, and Geothermal energy, which come either directly or indirectly from the sun, are almost considered to be environmentally friendly.

Solar power plants are the new topic in vogue these days. There are many different types of solar power plants which can be installed. PV power plant is the most common and widespread species of solar power plants and is generally categorized into off-grid and grid-connected systems.

Solar PV power plants usually utilize different PV technologies such as mc-Si, p-Si, amorphous silicon (a-Si), and other thin film technologies like copper indium di-selenide (CIS), copper indium gallium selenide (CIGS), and cadmium telluride (CdTe). However, the majority of the installed PV power plant types around the world have crystalline silicon (c-Si) technology.

* Corresponding author. Tel.: +98 34 3211 17 63; fax: +98 34 3212 09 64.

E-mail addresses: s.edalati@student.kgut.ac.ir, adalati.s@gmail.com (S. Edalati), ameri_mm@uk.ac.ir, ameri_mm@yahoo.com (M. Ameri), [\(M. Iranmanesh\).](mailto:m.iranmanesh@kgut.ac.ir)

During the last decade, grid-connected PV power plants have attracted more significant attention due to the advantage of their compatibility with the utility grid and efficient utilization in residential and industrial areas. In order to establish a grid-connected solar PV power plant or study the experimental output results of an installed one, it is necessary to consider and evaluate the performance of the most consequential factors, such as geographical location and meteorological data, PV modules and inverter characteristics, orientation and installation tilt angle, dust accumulation, humidity, and external shadings.

Over the last few years, various studies have been conducted on the performance parameters of installed PV power plants in different geographical locations, with different climatic conditions [1–15]. Performance analyses investigate the influences of PV module technologies, inverters, shading, wiring, array inclinations, tracking and fixed PV systems, type of grid connections, etc. on the overall performance of the PV power plant. The results of the performance analysis of a 1.4 kW roof top grid-connected photovoltaic power system under desertic weather conditions in Oman have been presented in the paper [16]. The performance ratio (PR) and capacity factor (CF) of the system were reported 84.6% and 21%, respectively. Pietruszko and Graczki [17] have investigated monitoring data from a 1 kW grid-connected PV system for a period of one year in Poland. They have reported the annual energy yield was about 830 kWh and the performance ratio ranged from 60% to 80%. Milosavljević et al. [18] reviewed the state-of-the-art solar energy potential and PV power plants in Serbia as well as similar studies around the world. They also performed an analysis of a 2 kW mc-Si grid connected solar PV power plant installed on the roof of the Faculty of Sciences and Mathematics (FSM building) in Niš, Republic of Serbia. The annual mean value of the PR and CF of the PV power plant were reported 93.6% and 12.88%, respectively.

Another experimental performance study is that of Wittkopf et al. [19]. In the frame of that study, the first zero-energy office building in Singapore used the 142.5 kWp p-Si grid-connected system on the roof of the building to meet its energy target. The first performance evaluation of the building-integrated PV system over 18 months of operation showed a good overall PR of 81%. Eke and Demircan [20] performed the performance analysis of a 2.73 kWp mc-Si PV power station under Mugla climatic conditions in Turkey.

The performance analysis of a fully monitored 171.36 kWp p-Si grid connected PV park in Greece has been conducted for the year 2007 on hourly, daily, and monthly bases. The authors [21] reported that the PV park supplied 229 MW h to the grid ranging from 335.48 to 869.68 kW h during 2007. PR varied from 58% to 73%, giving an annual PR of 67.36%. The final yield (Y_f) ranged from 1.96 to 5.07 h d⁻¹, and the average annual CF was 15.26%. Sharma and Chandel [22] explored the performance characteristics of a 190 kWp p-Si PV power plant in India and found that the maximum energy generated from the PV power plant is during March, September, and October and the minimum in January.

In the literature, there are also some studies which compare and investigate the performance of two PV power plants, simultaneously. A recent study is that of Congedo et al. [23], which focuses on the influence of climatic characteristics on a 960 kWp mc-Si PV power plant, divided in two subfields with different tilt angles and different nominal powers (606.6 kWp and 353.3 kWp) in south-eastern Italy. The results revealed that the performance ratio varies between 79% and 86.5% for the period of March to October 2012. Another relevant investigation is that of Al-Otaibi et al. [24]. They analyzed a twelve-month-long performance of the 80.05 kWp and 21.6 kWp CIGS grid-connected PV systems in Kuwait; the findings indicated that the performance ratio was maintained between 74% and 85% while the annual average daily final yield of the PV systems was 4.5 kW h/kWp day. On the other

hand, Micheli et al. [25] evaluated the performance of two grid-connected PV systems (17.94 kWp and 15.9 kWp) with different PV technology, rated power, and efficiency in northern Italy. The yearlong calculated performance ratio was 89.1% for the first PV system, which was equipped with mc-Si wafer surrounded by ultra-thin amorphous silicon layer (hetero-junction with intrinsic thin layer) and 82.7% for the second PV system, which was equipped with different kind of mc-Si PV modules. Further, in the paper [26] Tripathi et al. conducted a performance investigation for solar PV systems from mc-Si and a-Si grid-connected PV technologies in two 500 kWp solar PV power plants located at the same place in Gujarat, Western India. Performance analysis was done over an entire year; the PR of mc-Si ranged from 57.1% to 93.14%, and for a-Si it ranged from 53.72% to 87.64%. The final yield of mc-Si power plant ranged from a lower value of 2.79 h d⁻¹ to a maximum value of 5.14 h d⁻¹, and for a-Si power plant, it ranged from a lower value of 2.62 h d⁻¹ to a maximum value of 4.84 h d⁻¹.

At the present time, grid-connected PV power plants studies are interesting and informative, but based on the recent experimental studies, which are available in the literature [27–29] and to the authors' knowledge, there is still a lack of detailed performance analysis about mc-Si and p-Si PV module with almost similar electrical and mechanical characteristics. This paper aims to fill this gap by comparing the experimental behavior of these two common PV module technologies (mc-Si and p-Si) with exactly the same efficiency and maximum power at standard test conditions, the same mechanical properties, and almost similar in other electrical properties which experience the same fluctuations of solar irradiance and weather conditions. A series of field performances of these two PV module technologies in a grid-connected PV power plant in Kerman, Iran were consequently measured during twelve months to identify the more appropriate one.

2. PV-power plant description

The PV power plant is located at a latitude of 30°12'N, longitude of 56°52'E, and with an altitude of 1772 m above sea level in Khazra industrial park in Kerman, Iran with the monthly average daily values of solar radiation range from 3.86 to 8.28 kW h m⁻². An overall view of the power plant is given in Fig. 1.

The plant is installed on a gradual drop of a stony hill in two stairs. The top row is designed by mc-Si PV modules and the lower row is designed by p-Si PV modules. It is important to note that the results concerning the PV plant only are reported in this paper.

As can be seen in Fig. 1, two rows of PV arrays are installed on two stairs with a 3 m gap in such a manner that they do not cast a shade over each other. Seeing that the hill, on which the PV arrays are mounted, is high enough so that no shade is produced by surrounding buildings and trees. Fig. 2 indicates that the site layout is far away from any obstacles capable of shading over the arrays.

The PV power station is almost in the middle of the industrial park, and the surrounding regions have a semi-moderate and dry climate among semi-arid steppe lands (Fig. 2). Mani and Pillai [30] have suggested general recommendations to mitigate the impact of dust accumulation on PV performance according to climatic characteristics and conditions influencing PV performance. As they proposed weekly cleaning for PV modules in the steppe climate, there is a timetable for cleaning the power station modules by the use of weekly water jets. Using the excellent guidance of Mani and Pillai will prevent and mitigate the effect of soiling on the PV modules [9,31].

3. Design and selection consideration of PV power plant

In grid-connected PV power plants, the system is usually composed of the three main following components:



Fig. 1. Overall view of the 11.04 kWp solar photovoltaic plant in Khazra industrial park.

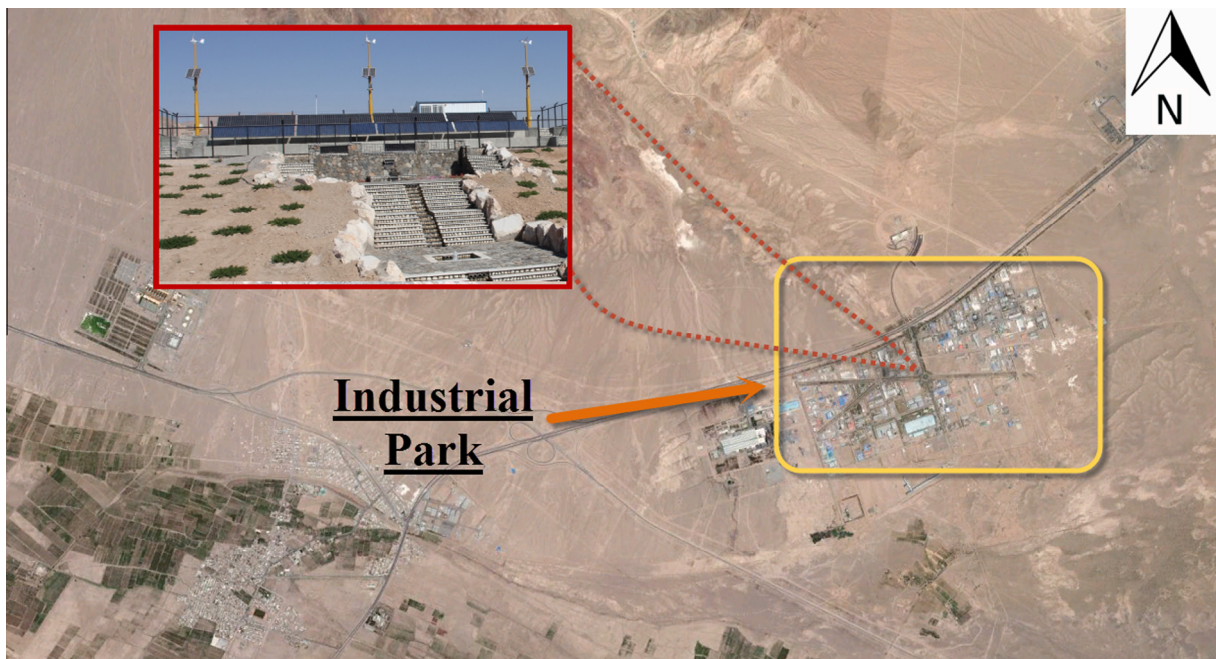


Fig. 2. Solar photovoltaic station map in Khazra industrial park.

- (i) PV modules
- (ii) Inverters
- (iii) Data measuring and monitoring devices

3.1. PV modules

The installed capacity of 11.04 kWp, grid-connected photovoltaic power station composed of two independent mc-Si and p-Si segments of 5.52 kWp in a proper series-parallel configuration, facing south and optimum monthly tilt angle to maximize monthly energy production. In this study, twenty-four mc-Si modules model LG230M1C and twenty-four p-Si module model LG230P1C are used with the same maximum power and efficiency. The electrical and mechanical properties of the modules are

summarized in [Table 1](#). There are four mounting structures of galvanized steel frame holding six modules for each type of modules. The design of the support structure would be such that the frame would keep a variable inclination with the horizontal plane. The structures have been designed with reinforced concrete foundation to withstand maximum wind speeds at the site as well as the modules weight.

[Fig. 3\(a\)](#) and [\(b\)](#) shows the $I-V$ and $P-V$ characteristic curves for mc-Si and p-Si at STC, respectively. [Fig. 3\(c\)](#) depicts that the $I-V$ and $P-V$ characteristic curves for mc-Si and p-Si are very close to one another. It should be noted that the similarity in $I-V$ and $P-V$ characteristic curves for mc-Si and p-Si modules at STC provides an expectation for the AC output power to be close in both of the mentioned PV modules.

Table 1
Electrical and mechanical properties of the PV modules.

Parameter	mc-Si	p-Si
<i>Electrical properties of the PV modules at STC^a</i>		
Maximum power (P_{\max})	230 W	230 W
Module efficiency (η)	14.3%	14.3%
Maximum power point voltage (V_{mp})	29.5 V	29.1 V
Current at maximum power point (I_{mp})	7.81 A	7.91 A
Open circuit voltage (V_{oc})	36.6 V	36.4 V
Short circuit current (I_{sc})	8.37 A	8.39 A
Module temperature at NOCT ^b (T_{NOCT})	43.8 ± 2 °C	45.7 ± 2 °C
Temperature coefficient of short circuit current ($\mu_{I_{sc}}$)	3.89 mA K ⁻¹	4.92 mA K ⁻¹
Temperature coefficient of open circuit voltage ($\mu_{V_{oc}}$)	-0.132 V K ⁻¹	-0.123 V K ⁻¹
Temperature coefficient of maximum power ($\mu_{P_{mp}}$)	-0.493% K ⁻¹	-0.456% K ⁻¹
Semiconductor bandgap ($E_{g,ref}$)	1.12 eV	1.12 eV
<i>Mechanical properties of the PV module</i>		
Cell number	6 × 10	6 × 10
Cell dimension	156 × 156 mm ²	156 × 156 mm ²
Module area	1.61 m ²	1.61 m ²
Operating temperature	-40 °C to +90 °C	-40 °C to +90 °C
Weight	19 kg	19 kg

^a STC (Standard Test Conditions): irradiance 1000 W m⁻², module temperature 25 °C, and air mass 1.5.

^b NOCT: irradiance 800 W m⁻², ambient temperature 20 °C, and wind speed 1 m s⁻¹.

The photovoltaic array is divided into four strings of twelve modules, each mounted in series. As shown in the schematic

diagram of the power plant in Fig. 4, each two independent strings are connected in parallel to an inverter.

The compatibility of this configuration with the inverters was carefully checked by a program in MATLAB [32] and the Sunny Design software (SMA, Germany). The two inverters were then connected to the local isolated grid running through the building downward; the power plant was powered by the grid forming unit.

3.2. Inverters

PV modules generate direct current (DC), which is converted into alternating current (AC) by inverters. An inverter is a device which feeds into the utility electrical grid by synchronized frequency (normally 50 or 60 Hz). Based on the maximum output power from each type of PV modules arrays, similar inverters are selected from SMA, model SunnyBoy 5000TL. The most relevant features of the inverter are tabulated in Table 2.

3.3. Data measuring and monitoring

The PV system is fully monitored with a SMA Sunny WebBox data logger integrated to a meteorological station and inverters through RS485 cables and record the data provided by various instruments. Table 3 exhibits the most relevant characteristics of the weather station. For the general data acquisition (DAQ), the global solar radiation, ambient and back temperature of the modules, DC array output power and AC array output, humidity, wind speed, and produced power in each array are recorded by the data logger and saved on a daily basis. The solar radiation reaching the PV modules is also measured by another

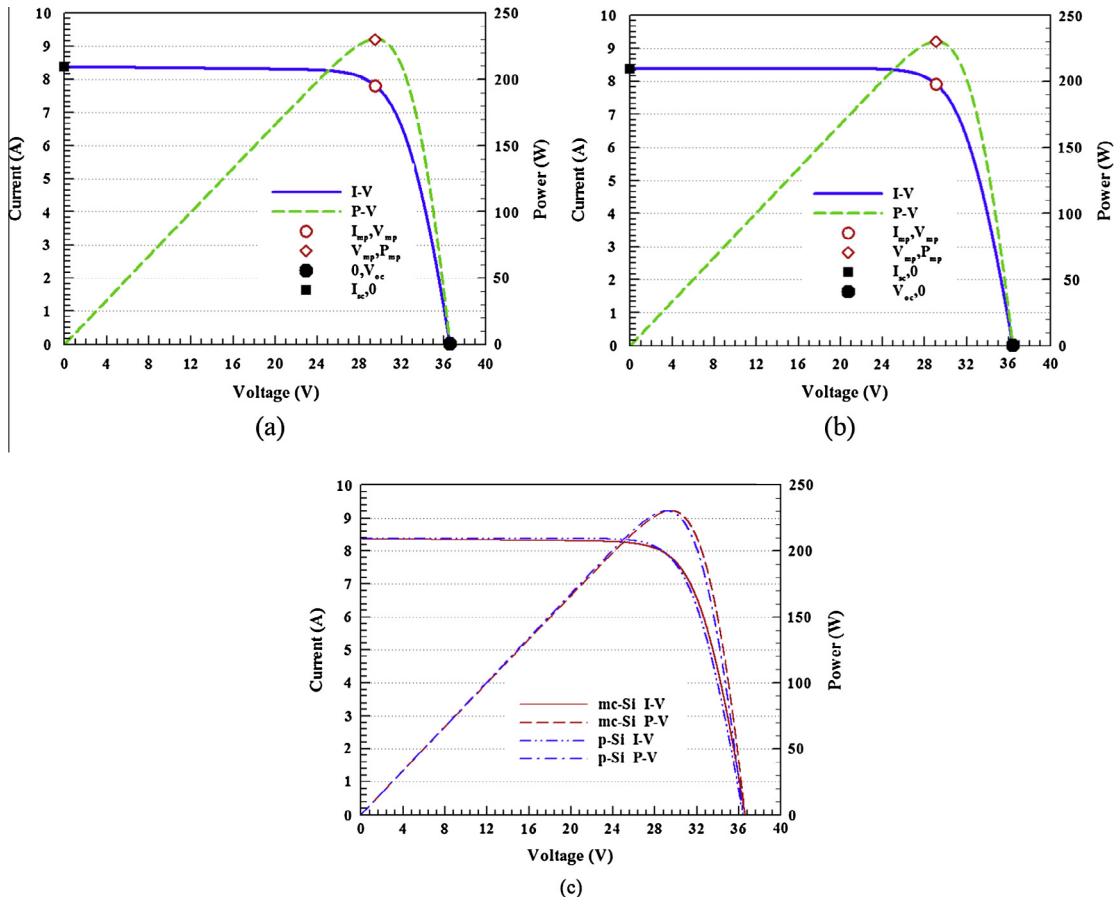


Fig. 3. The I - V and P - V characteristic curves for the PV module under STC conditions (a) mc-Si characteristic curves; (b) p-Si characteristic curves; (c) comparison between mc-Si and p-Si characteristic curves.

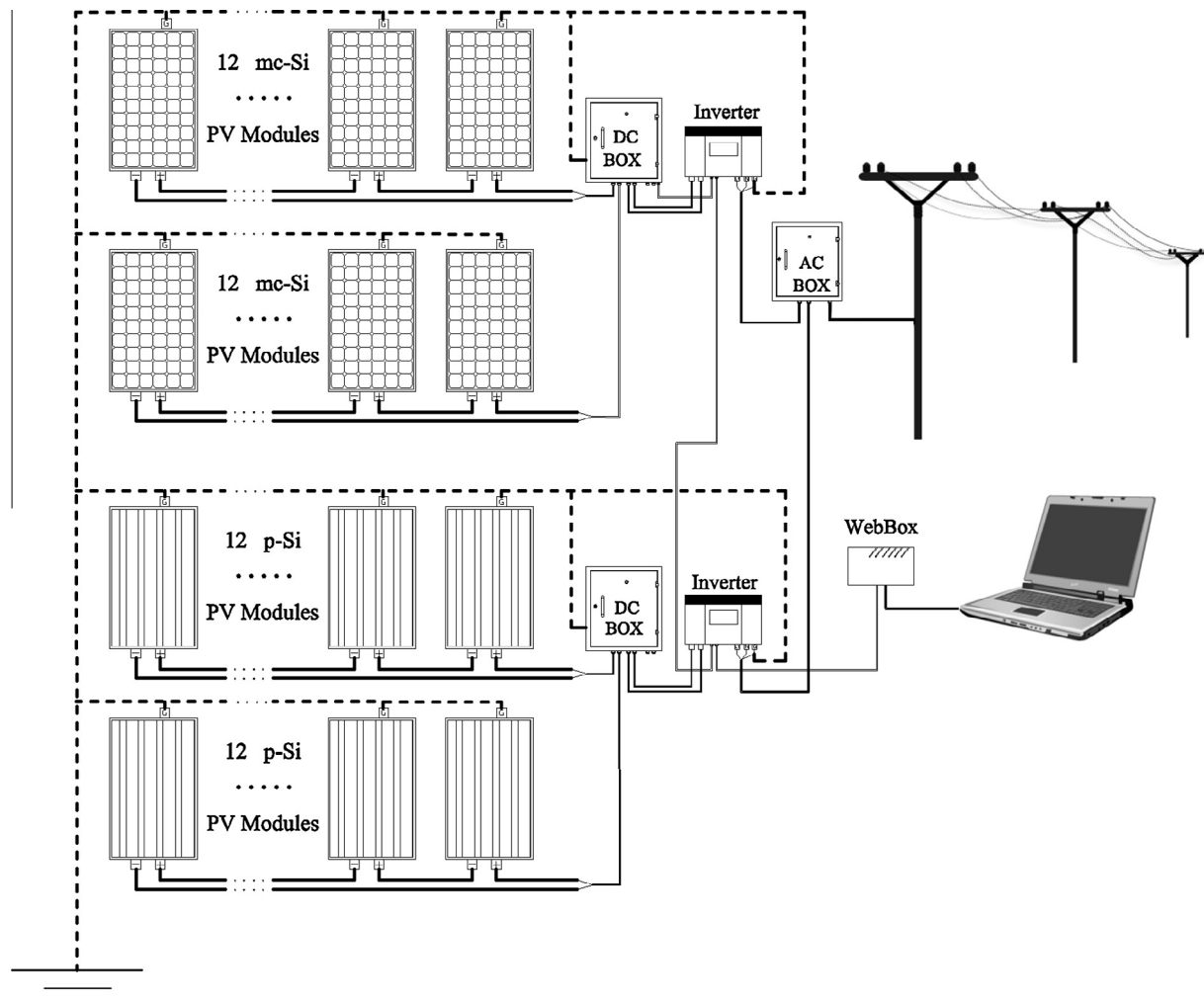


Fig. 4. Schematic diagram of solar photovoltaic station.

Table 2
Electrical properties of the inverters.

Input (DC)	
Max. DC power (@ $\cos \phi = 1$)	5250 W ³
Max. input voltage	750 V
MPP voltage range/rated input voltage	175–500 V/400 V
Min. input voltage/initial input voltage	125 V/150 V
Max. input current input A/input B	15 A/15 A
Output (AC)	
Rated power (@ 230 V, 50 Hz)	4600 W
Max. apparent AC power	5000 V A ²
Rated power frequency/rated grid voltage	50 Hz/230 V
Max. output current	22 A
Power factor at rated power	1
Max. efficiency/European weighted efficiency	97%/96.5%
General data	
Weight	26 kg
Operating temperature range	−25 °C to +60 °C
Noise emission (typical)	25 dB (A)
Self-consumption (night)	1 W
Topology	Transformerless
Cooling concept	Convection

measuring gage, placed on the same plane as that of the PVs. Thus, any shade, dirt and dust losses can be neglected since they are already included in the irradiance reaching the pyranometer. Inverters, Sunny WebBox, and monitoring system are placed in

the control room. Fig. 5 depicts the inside of the control room, which is equipped with a cooler system and a small exhaust fan to hold the inside temperature below +40 °C. This configuration forestalls the effect of temperature derating on inverter output and facilitates the heat dissipation from the inverter.

A small classroom is designed in the control room for enthusiastic students to study and discuss the PV power plant performances. All measured data from the devices are stored in a memory card inside the Sunny WebBox and are transmitted to a computer inside the control room once a month. In this paper, the sampling interval for simulation programs is set to 15 min, and the data recorded during the period from 1st July, 2013 to 30th June, 2014 will be used for the performance analysis of the PV power station.

4. Performance of the system

Accurate and reliable evaluation of any system performance is vital for a better designing of the system. In the PV industry, like many other systems, PV performance is an indicator of the quality of design and appropriate combination of PV equipment. International Electro-technical commission (IEC) presented the standard performance parameters for PV power systems as per IEC standard 61724 [33]. The most common performance parameters which provide a single base for comparing the PV power systems are summarized in Table 4.

Table 3

Technical characteristics of the weather station.

Pyranometer sensor
Measuring range: 0.0–1400.0 W m ⁻²
Resolution: <1 W m ⁻²
Spectral range: 300–2800 nm
Sensitivity: 5–20 μ V/W m ⁻²
Operating temperature rate: −40 °C to +80 °C
Maximum operational irradiance: 2000 W m ⁻²
Barometric pressure
Range: 300 hPa–1200 hPa (4.35–17.4 Psi)
Accuracy: ±1.5 hPa (±0.02 Psi)
Relative humidity
Range: 0–100% RH
Accuracy: ±2% RH
Air temperature
Range: −50 °C to +60 °C
Accuracy: 0.5 °C
Wind speed
Range: 0.8–40 m s ⁻¹
Accuracy: ±0.5%

^a Hectopascal is one of the common units of the pascal (1 hPa ≡ 100 Pa) which is equal to 1 mbar.

4.1. Final yield

The final yield is defined as the portion of the total energy generated (E_{AC}) by the entire PV power plant during a specified period of time (day, month or year) to the rated output power (P_{PV}) per kilowatt of installed PV array.

4.2. Reference yield

The reference yield is defined as the total in plane irradiance (H_t) divided by the reference irradiance (G_{STC}), which is 1 kW m⁻². This parameter represents the theoretical solar energy available for a defined period at any location where the PV power system is installed. Reference yield indicates the number of hours per day necessary for the solar radiation to be at reference irradiance levels in order to produce the same incident energy as was received by

Table 4

Overview of derived parameters for performance analysis.

Parameter ^a	Correlation	Unit ^b	Equation
Final yield (Y_F)	$E_{AC}/P_{PV, \text{Rated}}$	h d ⁻¹	(1)
Reference yield (Y_r)	H_t/G_{STC}	h d ⁻¹	(2)
Performance ratio (PR)	Y_F/Y_r	Dimensionless or %	(3)
Capacity factor (CF)	Y_F/hours	%	(4)

^a In this study performance parameters will be presented in monthly and yearly values.

^b The units h d⁻¹ can be expressed by: (kW h d⁻¹)_{Actual}/(kW)_{Rated}, precisely.

the PV modules. Both final yield and reference yield could have units of h m⁻¹ for monthly yield and h y⁻¹ for annual yield.

4.3. Performance ratio

Performance ratio is an important parameter independent of the PV power plant's geographical location with respect to irradiation. It indicates the ratio between actual and theoretical energy outputs of the PV power plant on a monthly or yearly basis. In grid connected PV system, higher values of performance ratio means the system is working at a more efficient operating point, and overall losses caused by wiring, inverter losses from converting DC to AC voltages, module temperature effects, module mismatch, and dust or snow on the rated output power are smaller. The closer the value of performance ratio to 100%, the more efficient the solar photovoltaic power plant operation. However, some factors, such as PV module temperature, solar irradiation, shade or dust on the PV module and pyranometer, location and condition of measuring sensors, efficiency of PV module and inverter, conduction losses due to the type and material of the cables, and differences in the technology of the PV modules and pyranometers influence the performance ratio value.

4.4. Capacity factor

Capacity factor is a purely definition-based parameter for electrical power plants which indicates the ratio of produced electricity



Fig. 5. Inside of control room of solar photovoltaic station in Khazra industrial park.

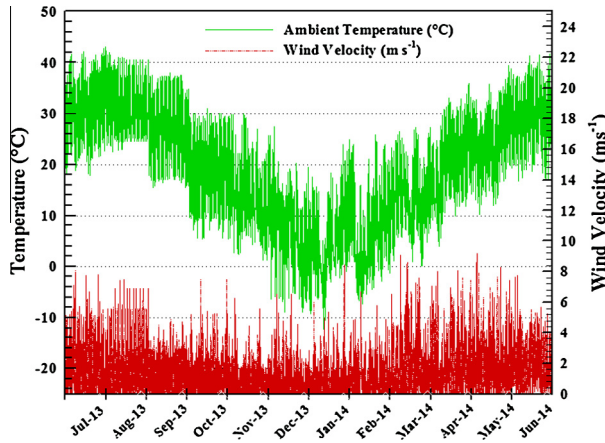


Fig. 6. Changes of ambient temperature and wind velocity for various months (above: ambient temperature; below: wind velocity).

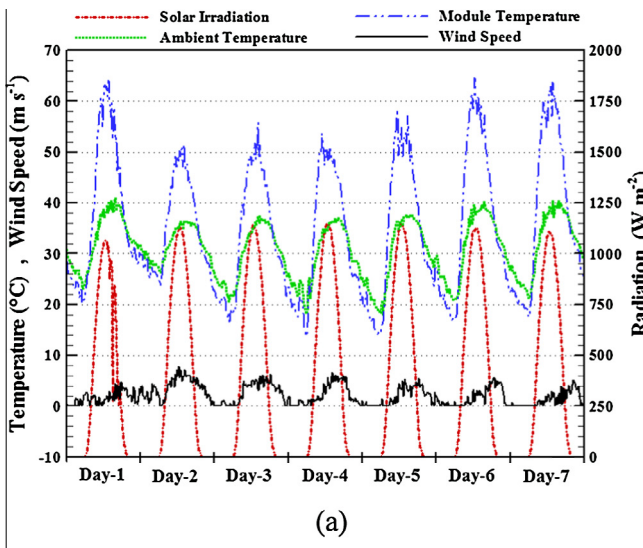
to the rated installed power for continuous operation during the same period of time. Nuclear power generations have the highest capacity factors while other fuels or technologies have the lower

capacity factor. Among clean and renewable energies, geothermal energy, and biomass operate at higher capacity factors in comparison to intermittent renewable sources like solar and wind, which tend to have lower capacity factors. Solar photovoltaic power plants usually have the capacity factors between 10% up to 30%, as their outputs fluctuate with the weather conditions and availability of the sun on daily or monthly basis.

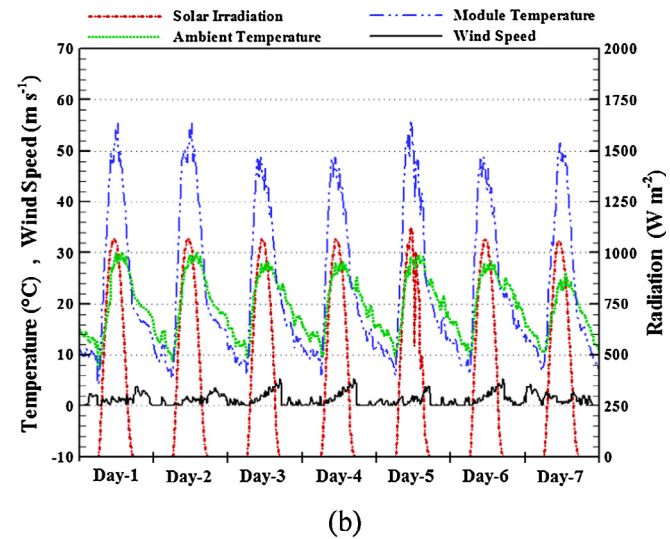
5. Data quality check

Data quality is the process of checking the measured data for consistency and other anomalies in the data (e.g. gaps), which is conducted in this study, based on the known parameter characteristics of the PV power station and meteorological conditions. According to the behavior of the PV power station and the environmental variables, a program in MATLAB software was coded to check the values of measured parameters to eliminate out-of-range measured data. The maximum and minimum allowable values for the parameters have been defined as below:

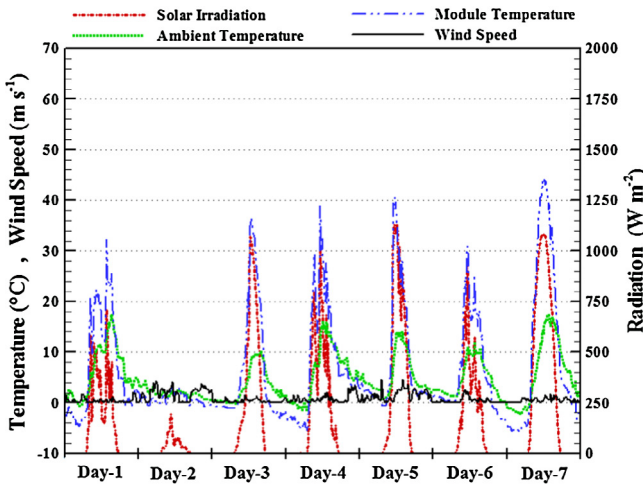
- Solar irradiance: between 0 and 1400 W m^{-2}
- Ambient temperature: between -20°C and 55°C
- Module temperature: between -25°C and 80°C



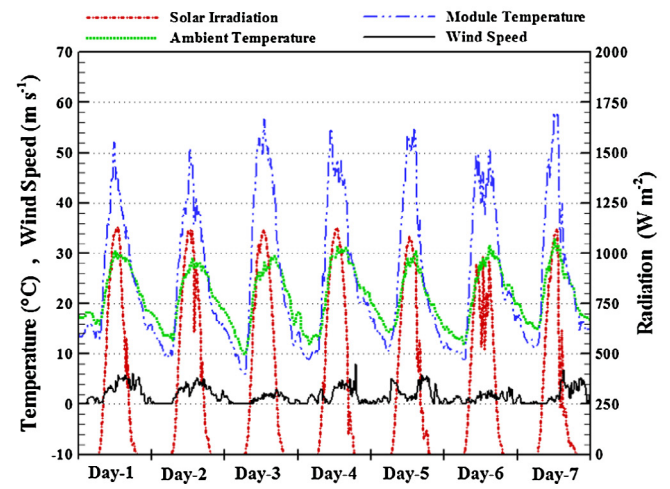
(a)



(b)



(c)



(d)

Fig. 7. Effects of ambient temperature, wind speed, and solar irradiation on mc-Si module temperature in different season (a) summer; (b) autumn; (c) winter; (d) spring.

6. Results and discussion

6.1. Meteorological dataset

In order to investigate the behavior of the PV power station, it is necessary to study the meteorological data recorded in the weather station. Fig. 6 shows the full data set, including ambient temperature and wind velocity during the operation period. The changes of ambient and module temperature during the selected period (twelve months consecutively) ranged from -12.5°C to 43°C , and -14°C to 68.5°C , respectively. The negative value of module temperature usually occurred during night time and in the absence of adequate solar radiation and output power production. During the measured period, monthly average daily wind velocity varied between 0.8 m s^{-1} in January and 2 m s^{-1} in July, relative humidity was less or equal to 97%, and the maximum value of global-tilt solar irradiation reached was 1225 W m^{-2} .

The measured ambient temperature, wind speed, solar irradiation, and the PV module temperature in an arbitrary week for each season are shown in Fig. 7(a)–(d) to illustrate the variation of each variable and its effect on module temperature.

From Fig. 7(a)–(d), it can be deduced that the module temperature is strongly affected by three main meteorological parameters, namely, the ambient temperature, solar irradiation, and wind velocity, in any optional day. It can be seen from Fig. 7(a)–(d) that module temperature commonly changes in patterns and positive difference value similar to ambient temperature during the operation process, even though it may come lower than the ambient temperature as a result of radiative cooling to the sky during clear sky at night time or at sunrises. As shown for a cold cloudy day in Fig. 7(c) (Day-2), the difference between ambient and module temperature significantly decreases in daytime due to the lack of appropriate solar irradiation on PV modules.

6.2. Performance of the PV power station

In order to assess the overall performance of PV power station configured as grid-connected, Eqs. (1)–(4) are used for all twelve months for mc-Si and p-Si PV modules and the results are shown in Fig. 8(a) and (b), respectively. From Fig. 8(a), the monthly average reference and final yield are deduced to be 197.49 h m^{-2} and 159.53 h m^{-2} , respectively; and according to Fig. 8(b), the average final yield for p-Si is 163.73 h m^{-2} , indicating a small increase in annual average output power for p-Si PV panels. From Fig. 8(a) and (b), it can be seen that even though the reference yield indicating the available solar energy is higher in spring and summer than in autumn and winter, but the monthly average final yield value is smaller in spring and summer in comparison to that in autumn and winter. The main reason for this large gap between reference and yield final in warm months should be the effect of excessive ambient temperature to the PV power generation. Thus, it can be inferred that higher values of performance ratio occur in cold months and lower values occur in warm months. Comparison of results for monthly average capacity factor of PV power station shows that it varies between 20% and 26% for mc-Si and between 20% and 27% for p-Si PV arrays.

In order to study the output power of mc-Si and p-Si arrays, a monthly comparison between performance ratio and capacity factor is conducted in parallel and the results are shown in Fig. 9. It can be seen from Fig. 9 that the performance ratio and also capacity factor have a slightly higher value for p-Si than mc-Si PV modules in each month. It is very important to investigate the causes of discrepancy of the performance ratios of PV c-Si. As mentioned in Table 1, both PV modules are selected with the same efficiency, and rated power under STC, but they have different temperature

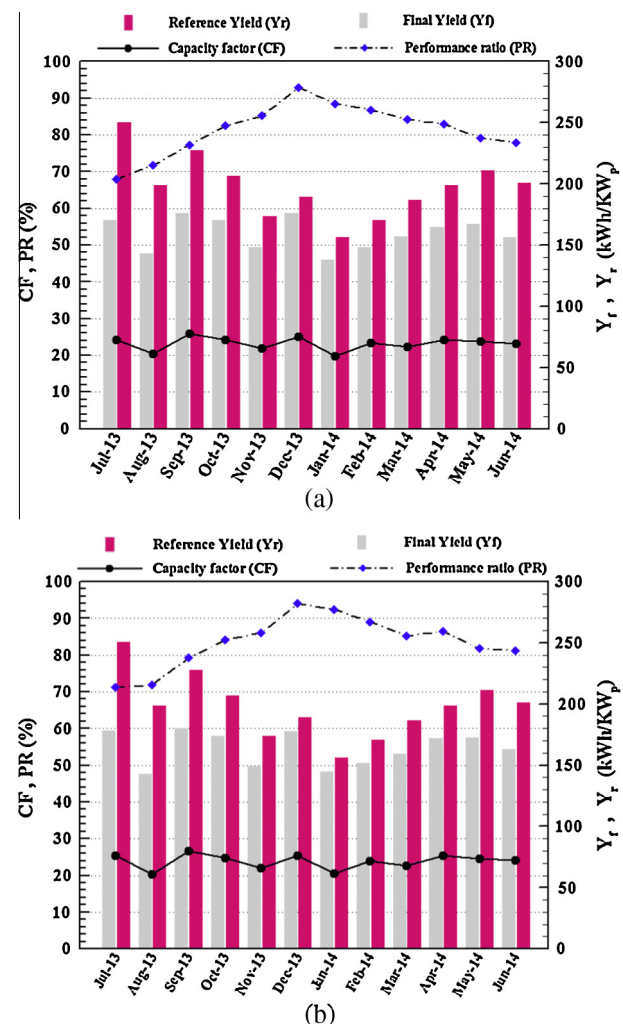


Fig. 8. Performance of the PV power station for PV array under real conditions during study period (a) mc-Si performance values; (b) p-Si performance values.

coefficients of power. Although the difference between I - V and P - V curves for c-Si modules is not very significant, as can be seen in Fig. 3(c), the temperature coefficient of power for mc-Si is

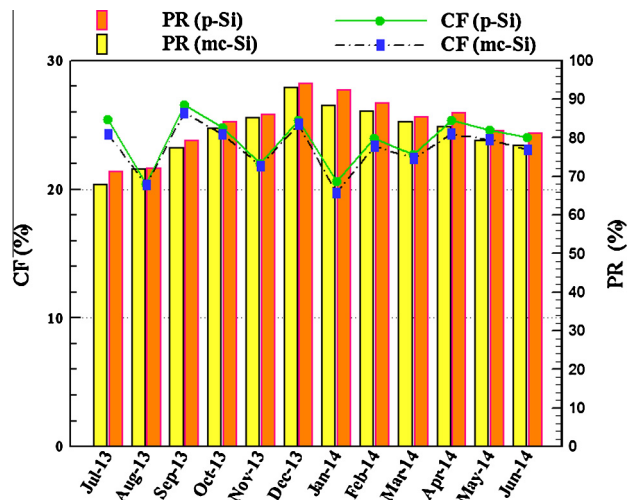


Fig. 9. Comparison between performance ratio and capacity factor for mc-Si and p-Si PV modules.

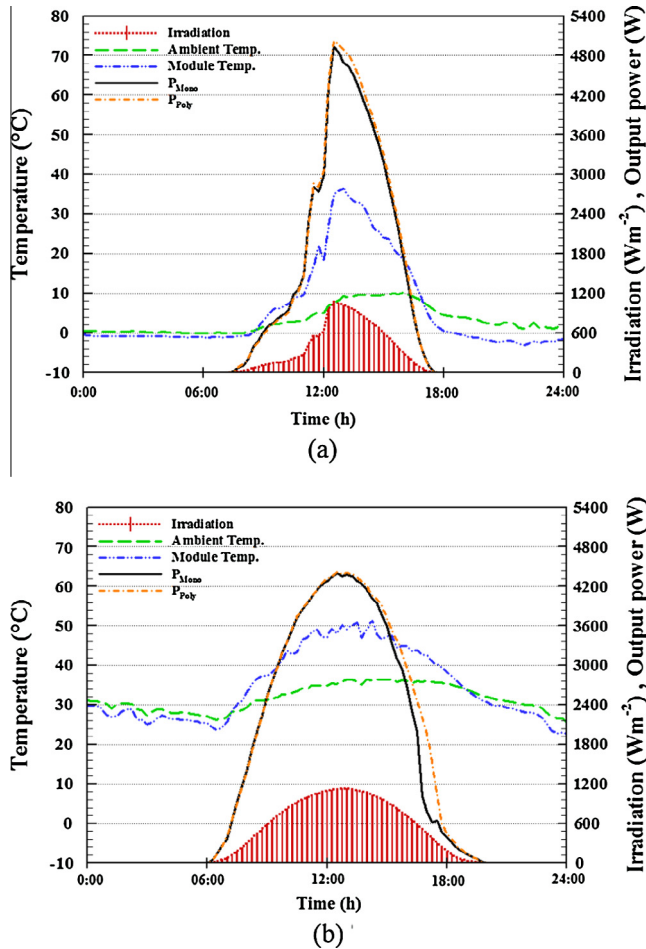


Fig. 10. Comparison between mc-Si and p-Si PV module output power in an arbitrary day (a) in winter; (b) in summer.

greater in comparison to its corresponding coefficient in p-Si PV module, which is about 8% in the negative value.

On this basis, it can be deduced that the consequence of an increase in module temperature is the decrease of the output power. Therefore, it can be concluded that the larger temperature coefficient of mc-Si PV modules compared to that of p-Si in this study leads to a decrease of the output power in the PV power station. The effect of larger value of ambient temperature is depicted in Fig. 10(a) and (b). As can be seen in Fig. 10(a) (a representative

day for winter), at low ambient temperature, the output powers of both mc-Si and p-Si are almost the same, whereas in higher ambient temperature, as shown in Fig. 10(b) (a representative day for summer), the output power of p-Si modules is larger than that of mc-Si PV modules.

7. Comparative performance of PV systems

In order to compare the obtained performance parameters of the PV power plant with the reported ones of other PV power plants at various climatic conditions [34] and geographical locations, a comparison is done in Table 5.

The annual average PR of the mc-Si modules in this study is lower than that of p-Si modules of monitored PV systems. However, it is higher than the ones reported in China, Greece, Poland, Singapore, and Turkey. The annual average daily final yields of mc-Si and p-Si modules in the PV power plant are 5.24 kW h/kWp day and 5.38, respectively and are higher than those reported in Table 5. The annual average CF of p-Si PV modules of the studied PV system is 23.81% while it is 23.20% for mc-Si PV modules. These both values of CF are eventually higher than those values for other mentioned studies in Table 5. It is worthy to note that the results obtained for the annual average of CF are in good agreement with that value reported in [35]. Besarati et al. proposed the very same value (equal to 23%) for CF in the location of this study according to a theoretical investigation using RETScreen software [36]. According to the mentioned definition of CF, the annual average of 23% can be construed as 2015 h or about 84 days in a year when the PV power plant is attainable to generate electrical energy at its nominal installed power.

8. Temperature-corrected performance ratio

As mentioned previously, the performance ratio depends on some factors. These effective factors can be generally classified in two main categories: (i) the efficiency of the system components and (ii) the weather characteristics.

The performance ratio dependence to the weather characteristics (especially the temperature) results in the problem of large seasonal variation in performance ratio [37]. Weather parameters which strongly affect the module temperature are wind, irradiance, and ambient temperature.

Accordingly, in order to solve the above problem, the performance ratio should be corrected to a reference module temperature (T_{ref}). This corrected PR is called “temperature-corrected performance ratio”, or PR^* and is calculated as follows [37–39]:

Table 5

Performance parameters of PV power plants in different locations.

Location	Climate zone ^a	Rated power (kWp)	PV module technology	Y_f (kW h/kWp day)	PR (%)	CF (%)	Energy yield (kW h/kWp)	Ref.
China	Temperate (Cfa)	3	p-Si	2.86	80.6	–	1063.04	[10]
India	Tropical (Aw)	20	p-Si	4.12	82	17.2	1507	[11]
Ireland	Temperate (Cfb)	1.72	m-Si	2.41	81.5	–	885.1	[12]
Greece	Temperate (Cs)	171.36	p-Si	1.96–5.07	67.36	15.26	1336.4	[13]
Malaysia	Tropical (Af)	5	p-Si	2.51	73.12	10.47	916.15	[14]
Norway	Cold (Dfb)	2.07	p-Si	2.55	83.03	10.58	931.6	[15]
Oman	Arid (BWh)	1.4	p-Si	5.1	84.6	21	1875	[16]
Poland	Cold (Dfb)	1	a-Si	2.3	60.8	–	830	[17]
Serbia	Temperate (Cfb)	2	mc-Si	3.18	93.6	12.88	1161.70	[18]
Singapore	Tropical (Af)	142.5	p-Si	3.12	81	–	1018.95	[19]
Turkey	Temperate (Cs)	2.73	p-Si	3.87	72	–	1414.18	[20]
Iran	Arid (BWk)	5.52	mc-Si	5.24	80.81	23.20	1914.4	Present study
Iran	Arid (BWk)	5.52	p-Si	5.38	82.92	23.81	1965.1	Present study

^a Climate data source [34].

Table 6

Comparison between traditional, STC, and NREL temperature-corrected performance ratio.

	mc-Si			p-Si		
	PR (%)	PR [*] _{STC} (%)	PR [*] _{NREL} (%)	PR (%)	PR [*] _{STC} (%)	PR [*] _{NREL} (%)
July-13	67.95	76.01	69.91	71.15	77.79	72.91
August-13	71.78	80.02	74.16	71.97	78.46	74.04
September-13	77.01	83.47	78.50	79.23	84.33	80.53
October-13	82.43	87.51	81.99	84.12	87.96	83.69
November-13	84.15	88.56	83.49	86.03	89.29	85.40
December-13	92.94	96.96	90.16	94.00	96.81	91.48
January-14	88.45	91.14	88.04	92.40	94.17	91.98
February-14	86.82	88.84	86.16	89.08	90.25	88.44
March-14	83.19	87.01	82.87	85.29	88.05	84.97
April-14	82.87	88.42	85.18	86.51	90.85	88.58
May-14	76.20	82.35	78.95	81.74	86.77	84.29
June-14	75.94	83.72	77.74	81.16	87.65	82.83
Average	80.81	86.29	81.52	82.92	87.14	83.52

$$\text{PR}^* = \frac{\text{PR} \text{ (equation 3)}}{1 - \left| \frac{\mu_{p_{mp}}}{100} \right| (T_m - T_{ref})} \quad (5)$$

where T_m is the temperature of the PV module.

Using $T_{ref} = 25^\circ\text{C}$ i.e. STC, gives PR^*_{STC} in a higher value in comparison to the traditional PR outlined in IEC 61724 because PV modules more frequently operate at higher temperature.

Thus, while correction to the STC temperature fundamentally solves the problem of PR seasonal variation, it may overestimate the actual performance which is not suitable for local climate assessments on PV systems.

In order to estimate PR^* more accurately, National Renewable Energy Laboratory (NREL) [37] has suggested the following equation which employs the average cell temperature of one year of weather data:

$$\text{PR}^*_{NREL} = \frac{\text{PR} \text{ (equation 3)}}{1 - \left| \frac{\mu_{p_{mp}}}{100} \right| (T_{cell-typ-avg} - T_{cell})} \quad (6)$$

where $T_{cell-typ-avg}$ is the average irradiance-weighted cell temperature computed from one year of weather data using the project weather file according to the Eq. (7) and T_{cell} is the operating cell temperature computed from measured meteorological data.

$$T_{cell-typ-avg} = \sum [H_{t_j} \cdot T_{cell-typ_j}] / \sum H_{t_j} \quad (7)$$

where j is indicated for each hour of the year (8760 h total).

In order to calculate the cell temperature, NREL suggests to use the Sandia precise model [40]. The Sandia model is presented in Appendix A. The operating cell temperature is representative for both ambient temperature and wind effects on PV modules operation. The results of comparison between traditional, STC, and NREL temperature-corrected performance ratio are tabulated in Table 6.

9. Conclusion

The present work provides the up-to-date data about the experimental behavior of a newly established grid-connected PV power plant under the semi-moderate and dry climatic conditions. The performance and experimental values of the mc-Si and p-Si PV modules with almost similar electrical and mechanical characteristics were measured, simulated, and analyzed during twelve months from July 2013 to end of June 2014 at the same time and in the same conditions. The conclusions obtained from the investigated results are as follows:

- As the ambient temperature, solar irradiation, and wind velocity have a high impression on the PV module temperature, the output power is strongly affected by the temperature of both

types of module technologies. However, the authors emphasize that the effects of humidity, dirt/dust, and wind velocity on the module temperature and output power from PV power plants should be studied simultaneously in order to obtain more accurate results.

- In comparing the selected mc-Si and p-Si PV module technologies with the same efficiency and maximum power, results show that p-Si PV modules produce more electricity, especially in higher ambient and module temperature. As p-Si PV modules are normally cheaper than mc-Si ones, authors suggest p-Si PV modules to be used in dry and warm regions like Iran. However, the impact of temperature coefficient of power should be considered in design and implementation of PV power plants.
- Highest final yield was recorded in September 2013 for both mc-Si and p-Si PV systems with monthly average of 175.95 kW h/kWp and 180.32 kW h/kWp, respectively; whereas lowest in January 2014 with monthly average of 138.21 kW h/kWp and 144.38 kW h/kWp, respectively.
- According to the obtained results and the fact that dry regions usually have appropriate solar radiation which is an essential factor for efficient performance of PV power plants, more attention should be paid toward implementing grid-connected PV power plants in suitable locations.
- The data provided in this study could be employed as a reference for further researches in planning and establish new grid-connected PV power plants and also would be useful in comparing energy yield of grid-connected PV power plants around the world.

Acknowledgements

The authors would like to gratefully acknowledge Kerman Regional Electric Company. Gratitude is also expressed to Kerman Industrial Parks Company for the assistance provided to access the measured data of the solar PV power plant.

Appendix A

Sandia proposed the following empirical correlation to calculate the PV module back temperature, T_m :

$$T_m = H_T \cdot (e^{a+bV}) + T_a \quad (8)$$

where a and b are parameters empirically determined and listed in Table A1 for different module types and mounting configurations of the module.

Once the PV module back temperature is determined, the cell operating temperature can be calculated as follows:

Table A1

Empirical coefficients to predict module back surface temperature.

Module type	Mount	a	b	ΔT_{cnd} (°C)
Glass/cell/glass	Open rack	-3.47	-0.0594	3
Glass/cell/glass	Close roof mount	-2.98	-0.0471	1
Glass/cell/polymer sheet	Open rack	-3.56	-0.0750	3
Glass/cell/polymer sheet	Insulated back	-2.81	-0.0455	0
Polymer/thin-film/steel	Open rack	-3.58	-0.1130	3
22X linear concentrator	Tracker	-3.23	-0.1300	13

$$T_{\text{cell}} = T_m + (H_t/G_{\text{STC}}) \cdot \Delta T_{\text{cnd}} \quad (9)$$

where ΔT_{cnd} is conduction temperature drop as presented in Table A1.

References

- [1] Zhou W, Yang H, Fang Z. A novel model for photovoltaic array performance prediction. *Appl Energy* 2007;84:1187–98. <http://dx.doi.org/10.1016/j.apenergy.2007.04.006>.
- [2] Kim J-Y, Jeon G-Y, Hong W-H. The performance and economical analysis of grid-connected photovoltaic systems in Daegu, Korea. *Appl Energy* 2009;86:265–72. <http://dx.doi.org/10.1016/j.apenergy.2008.04.006>.
- [3] Li DHW, Cheung KL, Lam TNT, Chan WWH. A study of grid-connected photovoltaic (PV) system in Hong Kong. *Appl Energy* 2012;90:122–7. <http://dx.doi.org/10.1016/j.apenergy.2011.01.054>.
- [4] Su Y, Chan L-C, Shu L, Tsui K-L. Real-time prediction models for output power and efficiency of grid-connected solar photovoltaic systems. *Appl Energy* 2012;93:319–26. <http://dx.doi.org/10.1016/j.apenergy.2011.12.052>.
- [5] Sharma V, Kumar A, Sastry OS, Chandel SS. Performance assessment of different solar photovoltaic technologies under similar outdoor conditions. *Energy* 2013;58:511–8. <http://dx.doi.org/10.1016/j.energy.2013.05.068>.
- [6] Padmavathi K, Daniel SA. Performance analysis of a 3 MWp grid connected solar photovoltaic power plant in India. *Energy Sustain Dev* 2013;17:615–25. <http://dx.doi.org/10.1016/j.esd.2013.09.002>.
- [7] Chemisana D, Lamnatou C. Photovoltaic-green roofs: an experimental evaluation of system performance. *Appl Energy* 2014;119:246–56. <http://dx.doi.org/10.1016/j.apenergy.2013.12.027>.
- [8] Khan F, Baek S-H, Kim JH. Intensity dependency of photovoltaic cell parameters under high illumination conditions: an analysis. *Appl Energy* 2014;133:356–62. <http://dx.doi.org/10.1016/j.apenergy.2014.07.107>.
- [9] Ferrada P, Araya F, Marzo A, Fuentealba E. Performance analysis of photovoltaic systems of two different technologies in a coastal desert climate zone of Chile. *Sol Energy* 2015;114:356–63. <http://dx.doi.org/10.1016/j.solener.2015.02.009>.
- [10] Wu X, Liu Y, Xu J, Lei W, Si X, Du W, et al. Monitoring the performance of the building attached photovoltaic (BAPV) system in Shanghai. *Energy Build* 2015;88:174–82. <http://dx.doi.org/10.1016/j.enbuild.2014.11.073>.
- [11] Kumar KA, Sundareswaran K, Venkateswaran PR. Performance study on a grid connected 20 kWp solar photovoltaic installation in an industry in Tiruchirappalli (India). *Energy Sustain Dev* 2014;23:294–304. <http://dx.doi.org/10.1016/j.esd.2014.10.002>.
- [12] Ayompe LM, Duffy A, McCormack SJ, Conlon M. Measured performance of a 1.72 kW rooftop grid connected photovoltaic system in Ireland. *Energy Convers Manage* 2011;52:816–25. <http://dx.doi.org/10.1016/j.enconman.2010.08.007>.
- [13] Bakos GC. Distributed power generation: a case study of small scale PV power plant in Greece. *Appl Energy* 2009;86:1757–66. <http://dx.doi.org/10.1016/j.apenergy.2008.12.021>.
- [14] Khatib T, Sopian K, Kazem HA. Actual performance and characteristic of a grid connected photovoltaic power system in the tropics: a short term evaluation. *Energy Convers Manage* 2013;71:115–9. <http://dx.doi.org/10.1016/j.enconman.2013.03.030>.
- [15] Adaramola MS, Vagnes EET. Preliminary assessment of a small-scale rooftop PV-grid tied in Norwegian climatic conditions. *Energy Convers Manage* 2015;90:458–65. <http://dx.doi.org/10.1016/j.enconman.2014.11.028>.
- [16] Kazem HA, Khatib T, Sopian K, Elmenreich W. Performance and feasibility assessment of a 1.4 kW roof top grid-connected photovoltaic power system under desertic weather conditions. *Energy Build* 2014;82:123–9. <http://dx.doi.org/10.1016/j.enbuild.2014.06.048>.
- [17] Pietruszko SM, Gradzki M. Performance of a grid connected small PV system in Poland. *Appl Energy* 2003;74:177–84. [http://dx.doi.org/10.1016/S0306-2619\(02\)00144-7](http://dx.doi.org/10.1016/S0306-2619(02)00144-7).
- [18] Milosavljević DD, Pavlović TM, Piršl DS. Performance analysis of A grid-connected solar PV plant in Niš, republic of Serbia. *Renew Sustain Energy Rev* 2015;44:423–35. <http://dx.doi.org/10.1016/j.rser.2014.12.031>.
- [19] Wittkopf S, Valliappan S, Liu L, Ang KS, Cheng SCJ. Analytical performance monitoring of a 142.5 kWp grid-connected rooftop BIPV system in Singapore. *Renew Energy* 2012;47:9–20. <http://dx.doi.org/10.1016/j.renene.2012.03.034>.
- [20] Eke R, Demircan H. Performance analysis of a multi crystalline Si photovoltaic module under Mugla climatic conditions in Turkey. *Energy Convers Manage* 2013;65:580–6. <http://dx.doi.org/10.1016/j.enconman.2012.09.007>.
- [21] Kymakis E, Kalykaklis S, Papazoglou TM. Performance analysis of a grid connected photovoltaic park on the island of Crete. *Energy Convers Manage* 2009;50:433–8. <http://dx.doi.org/10.1016/j.enconman.2008.12.009>.
- [22] Sharma V, Chandel SS. Performance analysis of a 190 kWp grid interactive solar photovoltaic power plant in India. *Energy* 2013;55:476–85. <http://dx.doi.org/10.1016/j.energy.2013.03.075>.
- [23] Congedo PM, Malvoni M, Mele M, De Giorgi MG. Performance measurements of monocrystalline silicon PV modules in South-eastern Italy. *Energy Convers Manage* 2013;68:1–10. <http://dx.doi.org/10.1016/j.enconman.2012.12.017>.
- [24] Al-Otaibi A, Al-Qattan A, Fairouz F, Al-Mulla A. Performance evaluation of photovoltaic systems on Kuwait schools' rooftop. *Energy Convers Manage* 2015;95:110–9. <http://dx.doi.org/10.1016/j.enconman.2015.02.039>.
- [25] Micheli D, Alessandrini S, Radu R, Casula I. Analysis of the outdoor performance and efficiency of two grid connected photovoltaic systems in northern Italy. *Energy Convers Manage* 2014;80:436–45. <http://dx.doi.org/10.1016/j.enconman.2014.01.053>.
- [26] Tripathi B, Yadav P, Rathod S, Kumar M. Performance analysis and comparison of two silicon material based photovoltaic technologies under actual climatic conditions in Western India. *Energy Convers Manage* 2014;80:97–102. <http://dx.doi.org/10.1016/j.enconman.2014.01.013>.
- [27] Sundaram S, Babu JSC. Performance evaluation and validation of 5 MWp grid connected solar photovoltaic plant in South India. *Energy Convers Manage* 2015;100:429–39. <http://dx.doi.org/10.1016/j.enconman.2015.04.069>.
- [28] Farhoodne M, Mohamed A, Khatib T, Elmenreich W. Performance evaluation and characterization of a 3-kWp grid-connected photovoltaic system based on tropical field experimental results: new results and comparative study. *Renew Sustain Energy Rev* 2015;42:1047–54. <http://dx.doi.org/10.1016/j.rser.2014.10.090>.
- [29] Mpholo M, Nchaba T, Monese M. Yield and performance analysis of the first grid-connected solar farm at Moshoeshoe I International Airport, Lesotho. *Renew Energy* 2015;81:845–52. <http://dx.doi.org/10.1016/j.renene.2015.04.001>.
- [30] Mani M, Pillai R. Impact of dust on solar photovoltaic (PV) performance: research status, challenges and recommendations. *Renew Sustain Energy Rev* 2010;14:3124–31. <http://dx.doi.org/10.1016/j.rser.2010.07.065>.
- [31] Fuentealba E, Ferrada P, Araya F, Marzo A, Parrado C, Portillo C. Photovoltaic performance and LCoE comparison at the coastal zone of the Atacama Desert, Chile. *Energy Convers Manage* 2015;95:181–6. <http://dx.doi.org/10.1016/j.enconman.2015.02.036>.
- [32] MATLAB V, 7.10. 0 (R2010a). MathWorks, Natick, MA; 2010.
- [33] Commission IE. IEC Standard 61724. Photovoltaic system performance monitoring guidelines for measurement, data exchange and analysis; 1998.
- [34] Peel MC, Finlayson BL, McMahon TA. Updated world map of the Köppen-Geiger climate classification. *Hydrol Earth Syst Sci* 2007;11:1633–44. <http://dx.doi.org/10.5194/hess-11-1633-2007>.
- [35] Besarati SM, Paddilla RV, Goswami DY, Stefanakos E. The potential of harnessing solar radiation in Iran: generating solar maps and viability study of PV power plants. *Renew Energy* 2013;53:193–9. <http://dx.doi.org/10.1016/j.renene.2012.11.012>.
- [36] RETScreen International: Renewable energy project analysis software. Minister of Natural Resources Canada; 2014. Available at: <<http://www.retscreen.net>>.
- [37] Dierauf T, Growitz A, Kurtz S, Cruz JLB, Riley E, Hansen C. Weather-corrected performance ratio. Technical Report, NREL/TP-5200-57991. National Renewable Energy Laboratory (NREL); 2013. Available at: <<http://www.nrel.gov/docs/fy13osti/57991.pdf>> [accessed 30 July 2015].
- [38] Nordmann T, Clavadetscher L, van Sark W, Green M. Analysis of Long-term performance of PV systems, different data resolution for different purposes, Report IEA-PVPS T13-05:2014. International Energy Agency (IEA); 2014. Available at: <<http://iea-pvps.org/index.php?id=305>> [accessed 30 July 2015].
- [39] Gostein M. Update on Edition 2 of IEC 61724: PV system performance monitoring; 2014. Available at: <http://www.nrel.gov/pv/pdfs/2014_pvmrw_84_gostein.pdf> [accessed 30 July 2015].
- [40] King DL, Kratochvil JA, Boyson WE. Photovoltaic array performance model. United States. Department of Energy; 2004. Available at: <<http://prod.sandia.gov/techlib/access-control.cgi/2004/043535.pdf>> [accessed 30 July 2015].